VOL. 10, NO. 4, MARCH 2015 ISSN 1819-6608
ARPN Journal of Engineering and Applied Sciences

www.arpnjournals.com

ARCHIMEDEAN SPIRAL ANTENNA ON MOVEABLE GROUND PLANE FOR UWB APPLICATIONS

AbdiRahman M. S., Fauziahanim C. S. and Waddah A.
Wireless and Radio Science Centre (WARAS), Faculty of Electrical and Electronic Engineering, University Tun Hussein Onn Malaysia Parit Raja, Johor, Malaysia
Email: shire_288@hotmail.com

ABSTRACT

In this paper we investigate the performance of a two-arm Archimedean spiral antenna over a moveable conducting ground plane (GP) for UWB applications. The performance of the antenna in terms of return loss, gain, axial ratio and radiation pattern are analyzed when the electrical separation between the spiral arm and ground plane is maintained at 0.25 λ over the frequency range 3.1 – 10.6 GHz. The results demonstrate that as physical separation of the GP reduces, the overall antenna's performance deteriorates. The results show that gain of the spiral antenna can be increased more than 9 dB with -10 dB operating bandwidth of more than 100%. The simulated and measured results have shown good agreements.

Keywords: UWB, ASA, ground plane reflector.

1. INTRODUCTION

There is a huge interest on designing a UWB antenna since the Federal Communication Commission (FCC) allowed 3.1-10.6 GHz unlicensed band for UWB communications or detection in 2002 [1]. Ultra Wideband is defined as any communication technology that occupies greater than 500 MHz of bandwidth, or greater than 25% of the operating center frequency [2] while most narrow band systems occupy less than 10% of the center frequency bandwidth, and are transmitted at far greater power levels. Challenges of the feasible UWB antenna design include the UWB performance issues of sufficient impedance matching bandwidth over wide frequency range (BW≤ 25%), high radiation efficiency (≤ 30%), a stable gain versus frequency response (more than 4dB), and good axial ratio (≥ 3 dB) [3, 4]. This makes an Archimedean antenna as a prime candidate for UWB circularly polarized systems.

A conducting backing plate is positioned 0.25 λ behind the spiral arm, so the ASA provides a unidirectional radiation pattern and a higher gain. Putting a fix conducting plate will destroys frequency independent characteristics since the electrical separation needs to maintain at 0.25 λ over the specified UWB frequency range [5]. This is also to preserve stable impedance matching and pattern distortion which impact on the maximum gain and axial ratio. Therefore, in this paper, the employment of moveable ground plane to retain 0.25 λ spacing at the specified frequencies is proposed in order to preserve the frequency independent characteristics of the ASA.

The design considerations of these structures are discussed in Section 2. In Section 3 the simulated reflection loss, gain, axial ratio and radiation pattern are plotted 3 different cases in which the moveable ground plane is adjusted to be 15 mm (Case 1), 11 mm (Case 2) and 7 mm (Case 3). Each configuration has electrical separation of 0.25 λ at 5 GHz, 6.85 GHz and 10.6 GHz respectively. Later, the simulated results are verified experimentally in Section 4.

ANTENNA DESIGN CONSIDERATION

Figure-1 shows the schematic design of a two-arm of the ASA which is simulated using CST Microwave Studio over frequency range 2 to 12 GHz. The frequency range was chosen so that the designed antenna able to cover the UWB frequency band. The width of the arm, w and the spacing between arms; s is designed to be the same so that a self-complementary antenna could be achieved. All parameters are calculated using equations in [6].

$$w = s = \frac{r_2}{4N+1} \quad (1)$$

$$r_2 = \frac{4.25\lambda_L}{2\pi} \quad (2)$$

Where N is the number of turns, r_2 outer radius and λ_L is the wavelength of the lowest frequency, 2 GHz. The arm width and spacing, inner radius, r_1 and r_2 is chosen to be 2 mm, 0.7 mm and 35 mm respectively. The number of turns of each arm is selected as 8 turns and the antenna was fed in anti-phase by using microstrip to parallel strip balun. The antenna was designed to generate right-hand circular polarization (RHCP) signals. The spiral arm is printed on 1.57 mm thick dielectric substrate of ε_r = 2.3.

The position, t of the ground plane is adjusted to be 15 mm (Case 1), 11 mm (Case 2) and 7 mm (Case 3) below the spiral arm so the air cavity provides 0.25 λ electrical thickness at the 5 GHz, 6.85 GHz and 10.6 GHz, respectively.

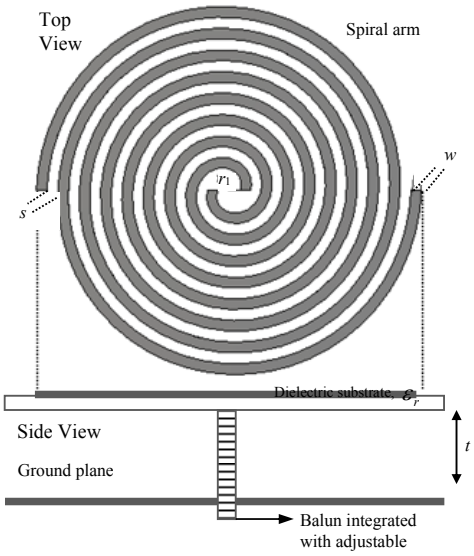

Figure-1. Schematic view of the ASA, substrate thickness; 1.57mm, r_1=0.7mm, r_2=35 mm, w=s=2mm.

SIMULATED RESULTS

The proposed spiral antenna was simulated in CST Microwave Studio using Time domain solver. The spiral arm was fed in anti-phase using microstrip to parallel strip balun. For all cases, ideally the electrical separation between the spiral arm and ground plane (air cavity) should be 0.25 λ so that perfect impedance matching occurs at the 5 GHz, 6.85 GHz and 10.6 GHz. However since the spiral arm was attached on 1.57 mm thick Rogers RT 5870 substrate with dielectric permittivity of 2.33, additional electrical thickness was incurred therefore the matching was slightly shifted downward. Figure-2 shows the simulated reflection loss for Case 1, Case 2 and Case 3. For Case 1, the structure provides -10 dB operating bandwidth of 139%. This values gradually reduces to 114% and 40% (defined between 8 GHz and 12 GHz) when the physical separation reduces to 11 mm and 7 mm. It is observed that the largest bandwidth of the three combinations is achieved in Case 1. The bandwidth improvement in Case 1 shows better performance compares to the previous work of spiral as in [8].

For Case 1, rapid signal fluctuations are observed below 3.3 GHz. The trend occurs for Case 2 (3.8 GHz) and Case 3 (5.5 GHz). For all cases the impedance mismatch reduces when the electrical separation is more than 0.17λ (As shown in Appendix 1). Whenever the ground plane is placed further away from the spiral arm, the mismatch highly reduces due to the reduction of the mutual coupling between the ground plane and the spiral arms [7]. A good impedance matching occurs when the electrical separation between the spiral arm and the ground plane is 0.25 λ (As shown in Appendix 1) where the S11 is given as -22 dB, and -28 dB. (Case 1 = 4.32 GHz, Case 2 = 5.6 GHz). The reflection loss increases gradually with frequency and the peak of 20 dB and 8 dB (Case 1 = 8.7 GHz, Case 2 = 11.3 GHz) occurs when the electrical separation is about 0.5λ (As shown in Appendix 1).

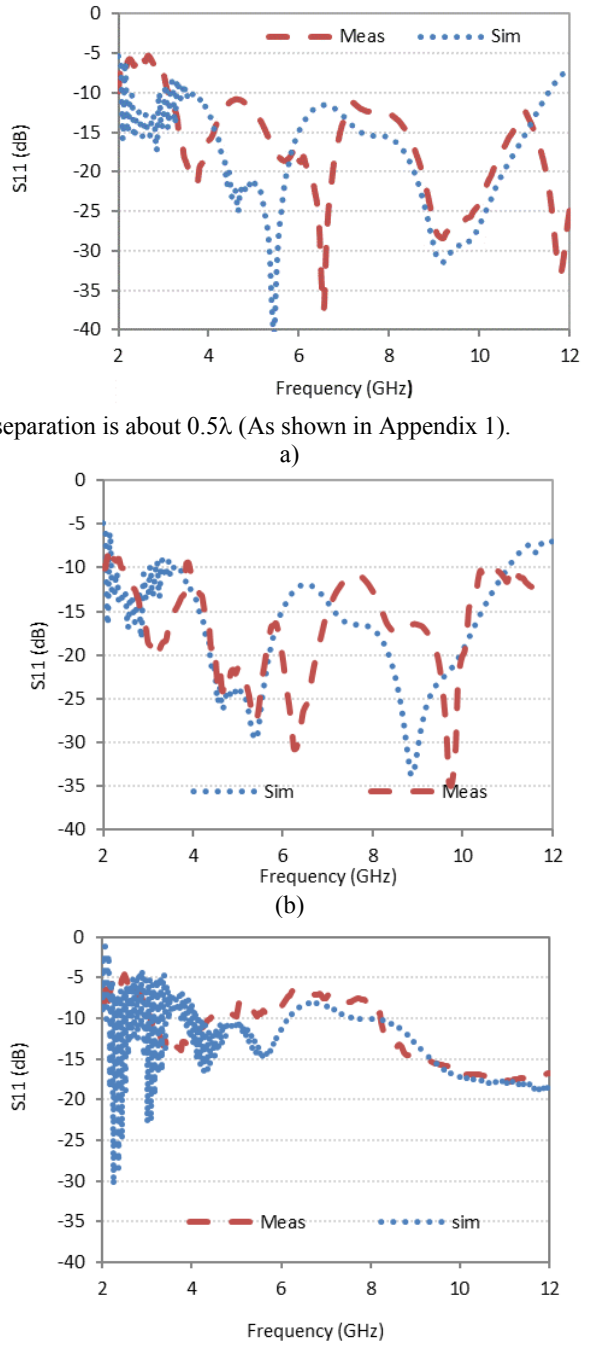

Figure-2. Comparison of measurement and simulated S11 at different ground plane position; (a) GP=15mm, (b) GP=11mm and (c) GP=7mm.

However the case is not applicable for Case 3 in which the S11 is -10 dB when the electrical separation between the spiral arms and the ground plane is 0.25 λ (As shown in Appendix 1) at 8 GHz and the reason why the case is not applicable at case 3 is due the physical size of the arm, which is big enough to provide modal

contamination. A good return loss performance of -20 dB continues until 12 GHz, in which the electrical separation is 0.38 λ (As shown in Appendix 1). Hence, still a considerable bandwidth of more than 40% (8-12 GHz), which is suitable for UWB applications is achieved.

However, case 3 shows smaller bandwidth (poor return loss performance) compared to cases 1 and 3 and The reason of the poor return loss is due to the ground plane which is close to the spiral arms, therefore, the ground plane surface has a 180^0 reflection phase and the image current (image current is the current of the image of spiral antenna, which is formed by the waves reflecting from the conductive ground plane) has an opposite direction to that of the original spiral. The converse image current wipes out the radiation of the antenna, bringing about an exceptionally poor return loss [9].

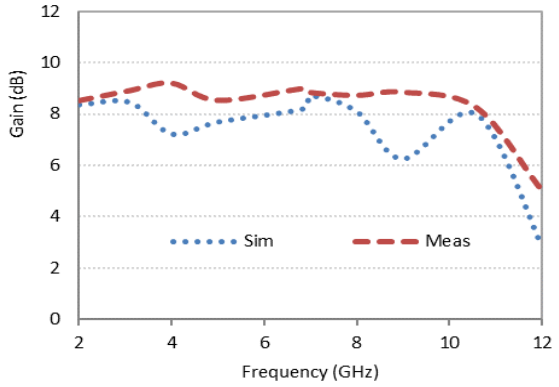

(a)

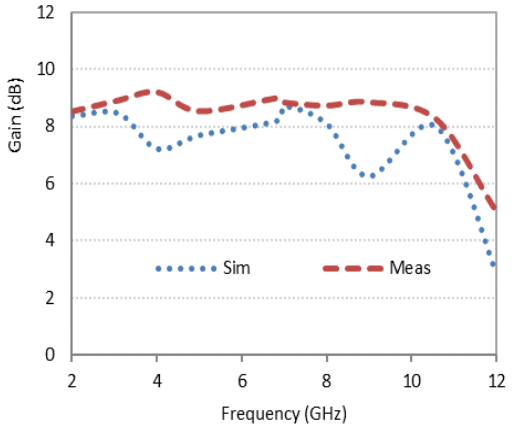

(b)

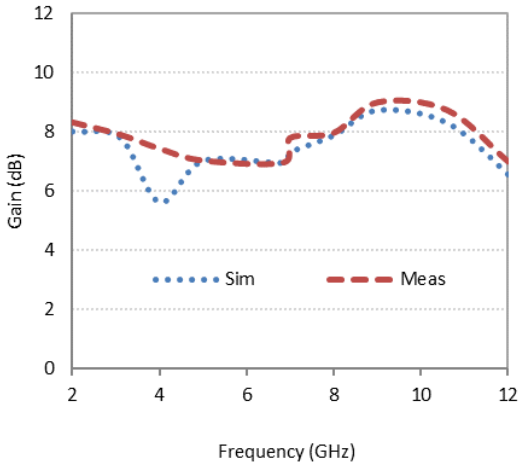

(c)

Figure-3. Comparison of measurement and simulated Gain at different ground plane position; (a) GP=15mm, (b) GP=11mm and (c) GP=7mm.

Similarly, high gain of up to 7.7 dB is achieved in case 1 when the electrical separation is 0.25 λ at 4.32 GHz as shown in Figure-3 (a). For Case 2, high gain of up to 7.8 dB is observed when the electrical separation is 0.25 λ at 5.6 GHz as shown in Figure-3 (b). In addition a gain of 7.9 dB is achieved in case 3 when the electrical separation is 0.25λ at 8GHz as it can be observed in Figure-3 (c). However, the gain decreases in cases 1 and 2 when the electrical separation is 0.5 λ because it can be seen that the gain is 6.6 dB at 8.7 GHz, 6.2 dB at 11.3 GHz in cases 1 and 2 respectively. While, in case 3, the gain is also expected to decrease when the electrical separation is 0.5 λ, which is beyond 12 GHz.

Therefore, in all the cases, the highest gain is achieved when the electrical separation between the spiral arms and the ground plane is 0.25 λ; this is due to the in-phase condition between the waves of the antenna and the ground plane [10]. While the gain decreases as the electrical separation becomes 0.5 λ. This is because the two waves are nearly canceling each other and a lower gain is achieved.

Likewise, an axial ratio of 2 dB, 2.5 dB and 3.2 dB is achieved in the cases 1, 2 and 3 respectively when the electrical separation between the spiral arms and the ground plane is 0.25 λ (Case 1 = 4.32 GHz, Case 2 = 5.6 GHz and Case 3 = 8.7 GHz) as indicated in Figure-4. Similarly, when the electrical separation increases to 0.5 λ the axial ratio of 0.8 dB and 4.2 dB is achieved at 8.7 GHz and 11.3 GHz in the cases 1 and 2 respectively. However, an electrical separation 0.5 λ of case 3 is beyond 12 GHz.

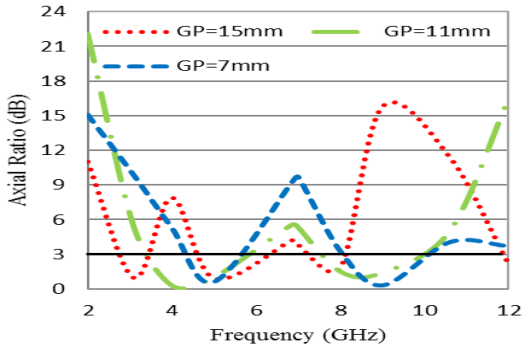

Figure-4. Comparison of Axial Ratio at GP different positions.

The radiation of the antenna is circularly polarized pattern when the axial ratio is less than 3 dB and the simulated circularly polarized radiation patterns at results at 3.1 GHz, 4 GHz and 9 GHz for GP at 15 mm, 11 mm and 7 mm respectively are discussed in Figure-5.

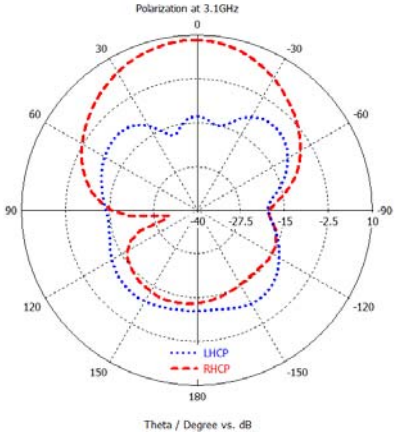

(a)

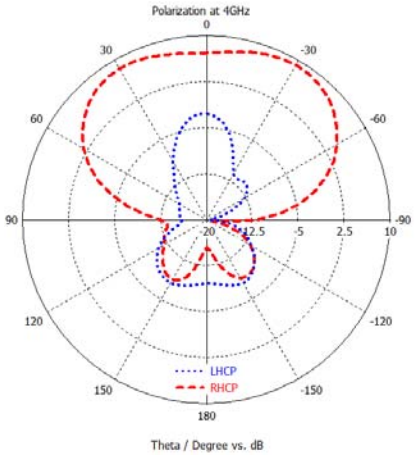

(b)

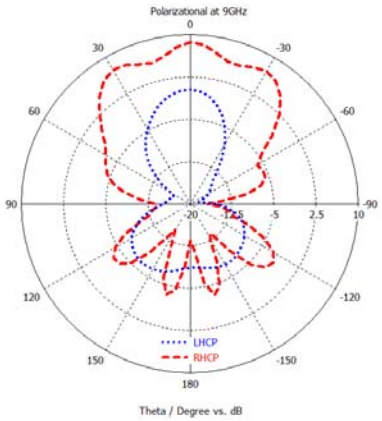

(c)

Figure-5. Circular Polarization at (a) 3.1GHz; GP=15mm, (b) 4GHz; GP=11mm and (c) 9GHz; GP=7mm.

Figure-5 presents performance Circular polarization of the radiation patterns for different frequencies such as 3.1 GHz, 4 GHz and 9 GHz. The co-polarization is the RHCP while the cross-polarization is the LHCP in each case of the patterns inFigure-5. The magnitude of the main lobe of LHCP is lower and its back lobes are higher compared to that of the RHCP. The reason is that the desired polarization of the spiral antenna is RHCP since the spiral antenna is fed at the center [12-14]. More details of the *absolute* patterns can be seen in Table-1.

Table-1. Details of the radiation pattern.

Frequency (GHz)	**GP Position** (mm)	**Main lobe Magnitude** (dB)	**Main lobe Direction** (angle)	**Angular width 3dB** (angle)	**Side lobe level** (dB)
3.1	15	9	4^0	78.7^0	-18.2
	11	8.7	17^0	98.1^0	-15.5
	7	8.3	24^0	104.4^0	-19.5
6.85	15	8.9	38^0	39.2^0	-2.2
	11	8.2	30^0	95.3^0	-7.7
	7	7	7^0	75.8^0	-11.7
10.6	15	7.7	13^0	20.7^0	-4.7
	11	8	50^0	51.7^0	-1.3
	7	8.3	39^0	116.7^0	-12

FABRICATION AND MEASUREMENT

The designed two arm Archimedean spiral antenna and microstrip to parallel strip balun are fabricated on substrates of Rogers RT 5870 which has permittivity of ε_r =2.33 and thickness of 1.57 mm. Substrate of low permittivity and small thickness is chosen because the use of low dielectric substrate permittivity or thin substrate can significantly improve its characteristics (return loss, gain, axial ratio and pattern) [6]. The fabrication process is performed using Photoetching process; in which, the

designed spiral antenna is printed on transparent film and then is exposed under UV light in order to cover the required region of the substrate. A developer solution is created so as to remove the photo-resist and then the antenna is placed in the etching tank in order to remove the unwanted copper. Finally, the antenna is rinsed and dried.

The measurement of scattering parameters of the antenna is carried out using vector network analyzer (VNA). The gain measurement of the spiral antenna was carried out by using a network analyzer and two identical horn antennas (1-18 GHz Double Ridge Horn Antenna).

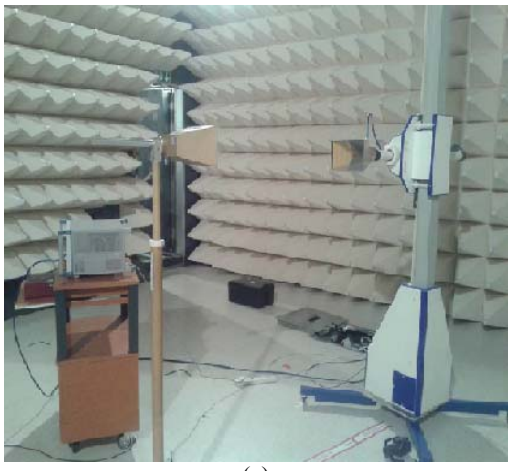

(a)

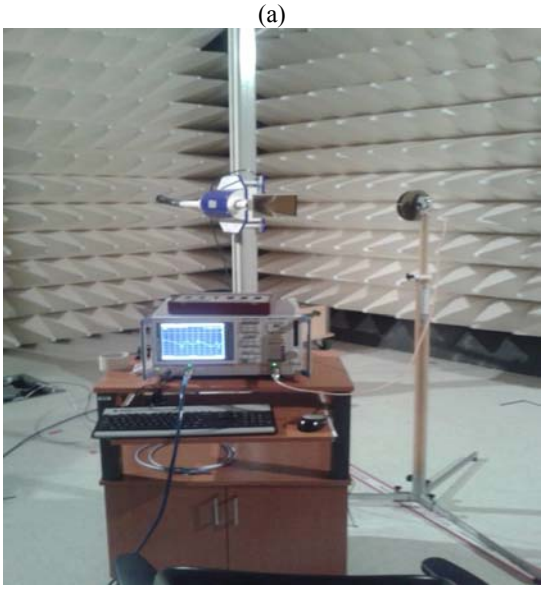

(b)

Figure-6. Gain measurement set up in the anechoic chamber; (a) for two Horn antennas and (b) for horn antenna and spiral antenna.

The most common for gain measurement methods are: absolute gain and gain comparison techniques [15]. In this paper, the gain comparison technique is used to measure for the spiral antenna's gain. In the gain comparison method, pre-known Standard Gain of Horn Antennas (1-18GHz Double Ridge Horn Antenna) are used to determine the absolute gain of the AUT (two arm Archimedean spiral antenna).

The comparison of the simulated and measured return loss of archimedean spiral antenna with various ground plane combinations are shown in Figure-2. Generally, it can be seen that in each case there is good agreement between the simulated and measured results of the return loss. In Figure-2 (a) and (b) it can be seen that the best return loss results are obtained when the ground plane is placed at 15 mm and 11 mm (λ/4 from 5 GHz and 6.85 GHz respectively) and the spiral antenna has more than 110% of bandwidth for the entire range of the working frequency at return loss better than -10 dB. On the other hand, it is presented that when the ground plane is placed at 7 mm (λ/4 from 10.6 GHz, see Figure-2 (c)) behind the spiral antenna, the antenna's measured return loss at lower frequencies is poor compared to the other cases.

Comparison of measurement and simulated gain at different ground plane positions are shown in Figure-3 (a) to (c). Same as the results of the return loss, it can be seen that in each case of Figure-3 (a) to (c), there is good agreement between the simulated and measured results of the gain. It can be seen in Figure-3 (a) the highest measured gain of 9.2 dB is obtained when the ground plane is placed at 15 mm (λ/4 from 5 GHz) behind the antenna. Figure-3 (b) and (c) show that the highest overall measured gain of the spiral antenna is 9 dB.

CONCLUSIONS

UWB Archimedean spiral antenna over a moveable conducting ground plane is analyzed. The parameters of the antenna are highly optimized using commercial software simulator; CST. It is investigated that as the height between the ground plane and the antenna is increased; antenna's performance improves and a large bandwidth of more than 130% and high gain of more than 9 dB are achieved when GP is placed at 15 mm behind the antenna. A good agreement between the measured and simulated results is shown.

ACKNOWLEDGEMENTS

The authors would like to thank Center for Graduate Studies of UTHM for their financial support and EMC center for their assistance with antenna measurements.

REFERENCES

[1] S. G. Mao., J. Ch. Yeh. and S. L. Chen. 2009. Ultra wideband circularly polarized spiral antenna using integrated balun with application to time-domain target detection. IEEE Transaction on Antennas and Propagation. 57: 1914-1920.

[2] D. Ghosh., A. De., M. C. Taylor., T. K. Sarkar., M. C. Wicks and E. L. Mokie. 2006. Transmission and

Reception by Ultra-wideband (UWB) Antennas. IEEE Antennas and Propagation Magazine. 48: 67-99.

[3] J. M. Bell and M. F. Iskander. 2004. A low profile Archimedean spiral antenna using an EBG ground plane. IEEE Transaction on Antennas and wireless Propagation. 3: 223-226.

[4] A. M. Abbosh. 2007. Gain and Bandwidth Optimization of Compact UWB Tapered Slot Antennas. International Journal of Microwave and Optical. 2(3).

[5] H. Nakano. and J. Yamauchi. 2010. Spiral antenna over composite HIS reflector" IEEE topics, APSURSI. pp. 1-4.

[6] A. M. Shire and F. C. Seman. Effects of dielectric substrate on the performance of UWB Archimedean spiral antenna. 2012. Proceeding of the 2013 IEEE International Conference on Space Science and Communication. (IconSpace). pp. 412-415.

[7] H. Nakano. and K. Nogami. 1986. A spiral antenna backed by a conducting plane reflector. IEEE Transaction on Antennas Propagation. 34: 791–796.

[8] P. H. Rao., M. Sreenivasan and L. Naragani. 2009. Dual Band Planar Spiral Feed Backed by Stepped Ground Plane Cavity for Satellite Boresight Reference Antenna Applications. IEEE Transactions on Antennas and Propagation. 57: 3752-3756.

[9] Y. Fan. 2009. Electromagnetic Band Gap Structures in Antenna Engineering, Cambridge University Press, New York, USA.

[10] Y. Fan and Y. Rahmat-samii. 2003. Reflection Phase Characterizations of the EBG Ground Plane for Low Profile Wire Antenna Applications. IEEE Transactions on Antennas and Propagation. Vol. 51, October.

[11] W. Baixiao. and A. Chen. 2008. Design of an Archimedean spiral antenna. Antennas Propagation and EM theory. pp. 384-351.

[12] F. J. Huang., T. Yo., C. Lee. and C. Luo. 2012. Design of Circular Polarization Antenna With Harmonic Suppression for Rectenna Application. IEEE Antennas and Wireless Propagation Letters. 11: 592-595.

[13] K. Woelders. and J. Granholm. 1997. Cross-Polarization and Sidelobe Suppression in Dual Linear Polarization Antenna Arrays. IEEE Transactions on Antennas and Propogation. 45: 1727-1740.

[14] C. W. Jung., B. A. Cetiner. and F. D. Flaviis. 2003. A Single-Arm Circular Spiral Antenna with Inner/Outer Feed Circuitry for Changing Polarization and Beam Characteristics. Antennas and Propagation Society International Symposium. 4: 474-477.

[15] IEEE Standard Test Procedures for Antennas, IEEE Standard 149TM, 1979, Reaffirmed December 10, 2008.

Appendix 1

Frequency (GHz)	**λ**	**ε in λ**	**cavity case 1**	**Electrical separation in λ**	**cavity case 2**	**Electrical separation in λ**	**cavity case 3**	**Electrical separation in λ**
0.5	6.00E-01	0.003994	0.02500	0.02899	0.01833	0.02233	0.01167	0.01566
1	3.00E-01	0.007988	0.05000	0.05799	0.03667	0.04466	0.02333	0.03132
1.5	2.00E-01	0.011983	0.07500	0.08698	0.05500	0.06698	0.03500	0.04698
2	1.50E-01	0.015977	0.10000	0.11598	0.07333	0.08931	0.04667	0.06264
2.5	1.20E-01	0.019971	0.12500	0.14497	0.09167	0.11164	0.05833	0.07830
3	1.00E-01	0.023965	0.15000	0.17397	0.11000	0.13397	0.07000	0.09397
3.5	8.57E-02	0.027959	0.17500	0.20296	0.12833	0.15629	0.08167	0.10963
4	7.50E-02	0.031953	0.20000	0.23195	0.14667	0.17862	0.09333	0.12529

4.3	6.98E-02	0.034350	0.21500	0.24935	0.15767	0.19202	0.10033	0.13468
4.32	6.94E-02	0.034510	0.21600	0.25051	0.15840	0.19291	0.10080	0.13531
4.5	6.67E-02	0.035948	0.22500	0.26095	0.16500	0.20095	0.10500	0.14095
5	6.00E-02	0.039942	0.25000	0.28994	0.18333	0.22328	0.11667	0.15661
5.5	5.45E-02	0.043936	0.27500	0.31894	0.20167	0.24560	0.12833	0.17227
5.6	5.36E-02	0.044735	0.28000	0.32473	0.20533	0.25007	0.13067	0.17540
6	5.00E-02	0.047930	0.30000	0.34793	0.22000	0.26793	0.14000	0.18793
6.5	4.62E-02	0.051924	0.32500	0.37692	0.23833	0.29026	0.15167	0.20359
7	4.29E-02	0.055918	0.35000	0.40592	0.25667	0.31259	0.16333	0.21925
7.5	4.00E-02	0.059913	0.37500	0.43491	0.27500	0.33491	0.17500	0.23491
7.9	3.80E-02	0.063108	0.39500	0.45811	0.28967		0.18433	0.24744
8	3.75E-02	0.063907	0.40000	0.46391	0.29333	0.35724	0.18667	0.25057
8.5	3.53E-02	0.067901	0.42500	0.49290	0.31167	0.37957	0.19833	0.26623
8.7	3.45E-02	0.069499	0.43500	0.50450	0.31900	0.38850	0.20300	0.27250
9	3.33E-02	0.071895	0.45000	0.52190	0.33000	0.40190	0.21000	0.28190
9.5	3.16E-02	0.075889	0.47500	0.55089	0.34833	0.42422	0.22167	0.29756
10	3.00E-02	0.079883	0.50000	0.57988	0.36667	0.44655	0.23333	0.31322
10.5	2.86E-02	0.083878	0.52500	0.60888	0.38500	0.46888	0.24500	0.32888
11	2.73E-02	0.087872	0.55000	0.63787	0.40333	0.49121	0.25667	0.34454
11.3	2.65E-02	0.090268	0.56500	0.65527	0.41433	0.50460	0.26367	0.35393
11.5	2.61E-02	0.091866	0.57500	0.66687	0.42167	0.51353	0.26833	0.36020
12	2.50E-02	0.095860	0.60000	0.69586	0.44000	0.53586	0.28000	0.37586